

Triggered Single-Photon Emission of Resonantly Excited Quantum Dots Grown on (111)B GaAs Substrate

Martin von Helversen, Alexey Vladimirovich Haisler, Marat Petrovich Daurtsev, Dmitry Vladimirovich Dmitriev, Alexander Ivanovich Toropov, Sven Rodt, Vladimir Anatolievich Haisler, Ilya Alexandrovich Derebezov, and Stephan Reitzenstein*

In the recent decades, semiconductor quantum dots (QDs) have proven to be valuable candidates as sources for various photonic applications. Of particular interest are, due to their wide-ranging applicability in quantum communication and computation, indistinguishable photons as well as entangled photon pairs, which can be emitted on demand. The latter require highly symmetric QDs with a small to vanishing excitonic fine-structure splitting. Herein, quantum optical properties of QDs grown via molecular-beam epitaxy (MBE) on (111)B-GaAs substrate are reported to study their emission in terms of triggered single-photon emission under quasi-resonant p-shell excitation, and under strict resonant s-shell excitation. The investigations reveal very good emission properties of these types of QDs, especially under s-shell resonant excitation. In fact, the results yield almost background-free triggered single photons with excellent multiphoton suppression associated with $g^{(2)}(0) = (0.033 \pm 0.027)$ and a degree of indistinguishability of $(41 \pm 10)\%$. The achieved results underline the high optical quality of (111)-QDs and show their high potential for applications in photonic quantum technologies.

1. Introduction

With the present development in the emerging field of photonic quantum technologies, including, for instance, exciting progress

in quantum key distribution,^[1–4] quantum teleportation,^[5,6] and boson sampling,^[7–10] the interest in high-performance single and entangled photon-pair sources is ever increasing. A variety of systems such as atoms, dye molecules, diamond color centers, semiconductor impurities, and quantum dots (QDs) have been used to demonstrate single-photon and entangled photon pair emission.^[11–17] Among them, self-assembled QDs are of particular importance due to their robustness and compatibility with semiconductor nanotechnology. Single QDs show sharp luminescence lines, high quantum efficiency, and excellent quantum properties.^[10,18–22] Regarding the optical properties it is important to note that in contrast to QDs on (001) GaAs substrate, for QDs grown on (111) GaAs substrate the piezoelectric field is directed along the growth direction [111] and does not lower

the symmetry below C_{3V} along the QDs base.^[23] As a result, they are expected to feature diminishing fine-structure splitting (FSS).^[23,24] This being a prerequisite for the generation of polarization-entangled photon pairs based on the radiative biexciton-exciton (XX-X) cascade,^[25] QDs grown on (111) GaAs substrate are attractive candidates for this application, as has been confirmed for (111)-grown pyramidal site-controlled QDs.^[14,26]

In the well-explored (001) GaAs material system, coherent control has proven to be a key component for high-quality photons leading to close to perfect values for the multi-photon suppression,^[27] as well as the generation of entangled photon pairs.^[15,16,20,28] The latter using either advanced and more challenging growth techniques, such as droplet-etching,^[29] or a rather complicated device design to control the QDs strain have to be applied.^[16,30] Furthermore, it is naturally desirable to enhance the outcoupling efficiency of the source. Popular approaches are the use of solid immersion lenses,^[19] which suffer from limited scalability, and micropillar cavities,^[31,32] the latter featuring a high quality, yet very narrowband enhancement, hindering the simultaneous coupling to the cavity of both XX and X due to typical finite binding energies of a few meV in InGaAs or GaAs-based QDs. Especially in recent years, circular Bragg gratings (CBG) have become a powerful alternative for overcoming the aforementioned issues,^[20,33–35] however demanding a high processing accuracy. Another well-established and efficient technique is the in situ integration of suitable QDs in monolithic microlenses.^[36] While

M. von Helversen, S. Rodt, S. Reitzenstein

Institut für Festkörperphysik

Technische Universität Berlin

10623 Berlin, Germany

E-mail: stephan.reitzenstein@physik.tu-berlin.de

A. V. Haisler, D. V. Dmitriev, A. I. Toropov, V. A. Haisler, I. A. Derebezov

Institute of Semiconductor Physics

Siberian Branch of Russian Academy of Sciences


630090 Novosibirsk, Russian Federation

M. P. Daurtsev, I. A. Derebezov

Institute of Telecommunications

Siberian State University of Telecommunications and Information Science

630102 Novosibirsk, Russian Federation

 The ORCID identification number(s) for the author(s) of this article can be found under <https://doi.org/10.1002/pssr.202200133>.

© 2022 The Authors. physica status solidi (RRL) Rapid Research Letters published by Wiley-VCH GmbH. This is an open access article under the terms of the Creative Commons Attribution License, which permits use, distribution and reproduction in any medium, provided the original work is properly cited.

DOI: 10.1002/pssr.202200133

integrating (111)-grown pyramidal site-controlled QDs in such nanophotonic structures is very challenging, it is straightforward to deterministically integrate (111)-QDs realized by droplet epitaxy into nanophotonic structures, such as microlenses.^[37]

In this work, we perform optical and quantum optical studies to explore the emission properties and quantum nature of single QDs grown on (111)-oriented GaAs substrate. The aim is to study the optical quality of such QDs and to evaluate their potential for applications in advanced photonic quantum technologies relying on high multiphoton suppression and photon indistinguishability. For this purpose, we optimized the epitaxial growth of (111) QDs with a backside distributed Bragg reflector (DBR) and applied quasi-resonant (p-shell) as well as strict resonant coherent s-shell excitation to determine the multiphoton suppression and the photon indistinguishability of these quantum emitters with typically small fine structure splitting.

2. Sample and Experimental Setup

2.1. Sample Design

The layer and device design were numerically optimized by the finite element method (FEM) approach to maximize the photon extraction efficiency η_{ext} . In the design studies, we chose the microlens concept as a robust and material-independent approach to increase η_{ext} which is well established for InGaAs QDs on (001) GaAs substrate,^[36] and has recently also been realized for (111) InGaAs QDs.^[37] However, focusing mainly on the optical properties of the QDs and not so much on maximizing the photon extraction efficiency, in the present work only planar, as-grown samples were studied. This also facilitates optical studies under strict-resonant excitation because of better stray-light suppression. Following the numerically obtained design rules,

the sample was grown by MBE on n-doped (111)B GaAs substrate, with a miscut of 2° in the [211] direction. The full epitaxial structure (see **Figure 1**) consisted of a lower DBR mirror, which is followed by a 467 nm thick GaAs layer containing a (111) InGaAs QD layer 400 nm below the sample surface. The self-assembled QDs were grown by droplet epitaxy and the DBR is formed of 23 periods of alternating $\lambda/4$ -thick layers of GaAs and $\text{Al}_{0.9}\text{Ga}_{0.1}\text{As}$. The ≈ 100 nm wide stopband of the DBR is centered at 930 nm and provides close to unity reflection ($R > 0.99$) at the QD emission wavelength range.

2.2. Experimental Setup

As shown in Figure 1, the sample was mounted in a closed-cycle cryostat and was temperature stabilized at 5 K. A stack of piezo-based nano-positioners allowed 3D movement with nm accuracy. A single aspheric lens ($f = 3.1$ mm, $\text{NA} = 0.77$) was integrated into the inner cold shield of the cryostat and used to focus the excitation laser as well as to collimate the sample's microphotoluminescence (μPL). The μPL signal was then collected by an $f = 18$ mm aspheric lens and coupled into a single-mode fiber (Thorlabs 780 HP), which also serves as a spatial filter for resonant excitation (the core of the fiber with a mode-field diameter of $\approx 5 \mu\text{m}$ was imaged by the aspheric lens to a circle of about 800 nm in diameter on the sample surface).

For spectral analysis, a free-space spectrometer ($\approx 25 \mu\text{eV}$ full width at half maximum (FWHM) resolution) was available, which can also be used for spectral selection using its exit slit. Alternatively, simply a bandpass filter (10 nm width, centered at 930 nm) was employed. The filtered signal was fed into a single-mode fiber-based Hanbury Brown and Twiss (HBT) setup with two Si avalanche photon diode (APD) based single-photon counting modules (SPCMs) for the autocorrelation

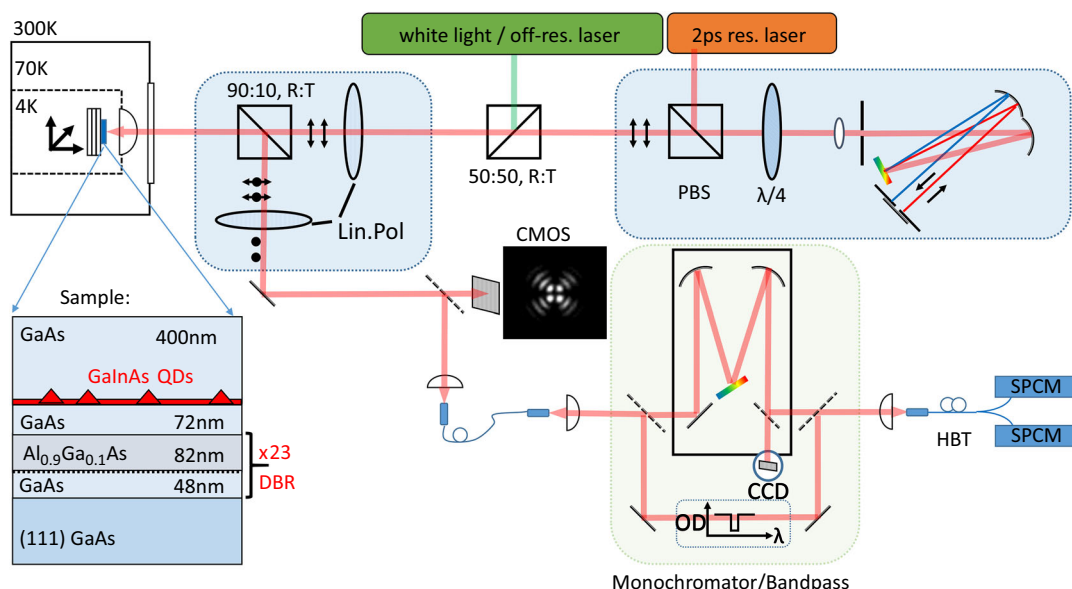


Figure 1. Sketch of the experimental setup and layout of the sample structure. The emission of a 2 ps pulsed laser (FWHM 0.7 nm) is spectrally narrowed using the exit slit of a 1200 L mm^{-1} monochromator. A second beam-splitter (50:50) allows for coupling of white light as well as for off-resonant pumping (780 nm continuous wave (cw)). For s-shell excitation, a scheme of polarization-suppression is used, and the fiber-coupled signal can be spectrally filtered (monochromator/bandpass/no filtering) before the time-correlation is recorded.

measurements (combined time resolution: ≈ 500 ps). Off-resonant excitation was provided by a continuous wave diode laser at 785 nm, while p-shell or s-shell resonant excitation is carried out with a 2 ps pulsed tunable optical parametric oscillator (OPO) laser (repetition frequency 80 MHz). For resonance fluorescence measurements two Glan–Thompson-type polarizers are added to the setup to suppress the backscattered laser. By angular fine-adjustment using two piezo rotation mounts, a total extinction ratio in the single-mode fiber of $>5 \times 10^6$ can be reached and $>1 \times 10^6$ held stably for multiple hours.^[38] The ps-pulsed laser source used for resonant excitation is spectrally much broader (≈ 0.7 nm) than the addressed QD transition. For this reason, a pulse-slicing apparatus via a 1200 L mm^{-1} grating, two focusing mirrors ($f = 0.3$ m), and a mechanical slit, which blocks other than the selected frequencies, was employed. A mirror placed within the Rayleigh length of the beam at this exit slit sends the light back through the same monochromator to compensate for the geometric path difference of the selected frequencies and was separated from the input beam via its polarization using a quarter-wave plate and a polarizing beam splitter. For resonant excitation, a spectral pulse width of 0.1 nm (FWHM) was used. This pulse-slicer is not a 4f-line as found in zero-dispersion pulse-shapers, but rather adds a positive group velocity dispersion (GVD) to the pulse, which has been shown to allow for adiabatic rapid passage in QD two-level systems,^[39] rather than the well-known Rabi oscillations.^[10,19,20,22,39–42]

3. Results and Discussion

We first choose a single QD emitting at about 930 nm, whose off-resonant (785 nm, cw) characterization is shown in **Figure 2**. The PL under this excitation presents three bright emission lines (indicated in Figure 2a), which are further characterized by the use of power- and polarization-dependent studies (depicted in Figure 2b,c, respectively). The latter reveal a clear anti-oscillatory behavior of the emission energies of two states due to a rather large (FSS) of $(14.9 \pm 0.1) \mu\text{eV}$ compared to typical values below $10 \mu\text{eV}$ for this type of QDs.^[37] This allows for a quick and clear identification of the neutral exciton and biexciton as well as a singly charged exciton, showing no polarization-dependence of its emission energy. The identification of states is also confirmed via the power-dependent PL (Figure 2b). For quasi-resonant (strict resonant) excitation into the p-shell (s-shell) of the QD, we focus on the charged exciton at 1.3384 eV, as this transition is easily populated in all three used excitation schemes, and therefore allows for a direct comparison. We attribute the nonvanishing fine-structure splitting in this type of sample to geometrical deviations from spherical QDs, possibly favored by the aforementioned 2° miscut of the crystal along the [211] direction.

By means of pulsed micro photoluminescence excitation (μPLE), the p-shell transition of the QD is found at 905.9/906.6 nm (1.3675 eV), which equals an s-p-splitting of about 20 nm (29 meV) as shown in Figure 3a. The second-order auto-correlation measurement (Figure 3b) reveals single-photon emission with a value of $g^{(2)}(0)_{\text{fit,p-shell}} = 0.12 \pm 0.02$. The peak function in the fit is based on a monoexponential decay, which was convoluted with the time resolution of the setup.

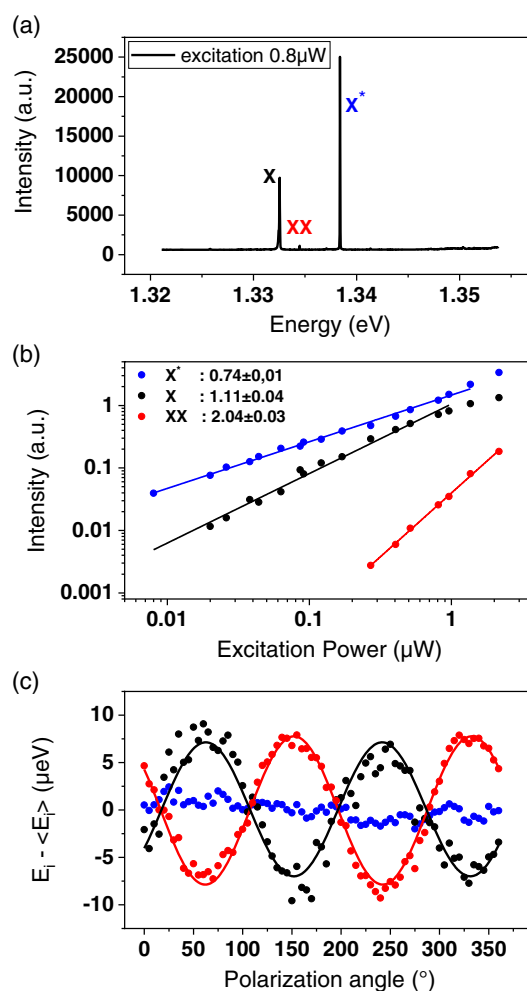


Figure 2. Emission properties of the studied (111)-quantum dot under off-resonant (785 nm) CW excitation. a) Micro-photoluminescence spectrum at an excitation power of $0.8 \mu\text{W}$. The observed emission lines are attributed to the neutral exciton X, the neutral biexciton XX, and a charged exciton X^* . b) Excitation power-dependent μPL intensity of the three states shown in a). The fit to the data in double logarithmic scaling is shown in solid lines and the slopes are indicated. c) Linear polarization dependence of the respective central energies. For better visibility, the energies are normalized with respect to their mean. The FSS of $(14.9 \pm 0.02) \mu\text{eV}$ is obtained by a sinusoidal fit.

For strict resonant excitation, the pulsed laser is tuned to the energy of the addressed transition as shown in Figure 3c. Interestingly, even though the QD features a clear and stable p-shell, in this excitation scheme the resonance fluorescence (RF) is strongly enhanced by adding a weak off-resonant laser or, equally efficient, some off-resonant white light to the excitation. Either of these two methods does not contribute to any measurable emission from the desired transition even at integration times of the charge coupled device (CCD) camera larger than 5 s. However, some luminescence of other QDs and/or white light is still coupled into the detection fiber, as shown in the autocorrelation results in the following. We attribute the positive effect of the off-resonant white light to a stabilization of the electronic potential landscape in the direct vicinity of the QD.^[43,44] As

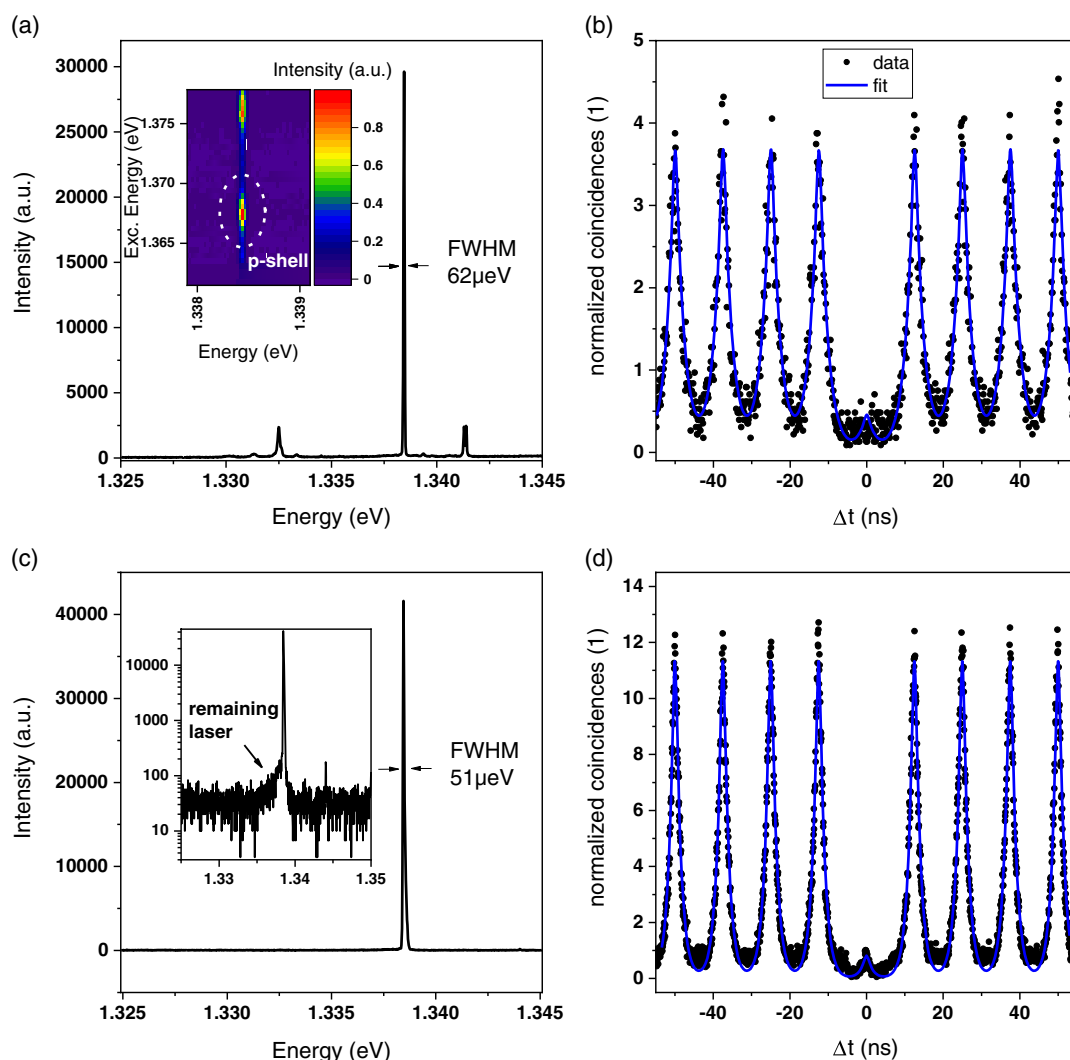


Figure 3. Emission properties of the studied (111)-QD under pulsed excitation. a) μ PL spectrum under pulsed (2 ps) p-shell excitation (905.5 nm) in saturation of the charged excitonic state at an excitation power of 5 μ W. The inset shows a pulsed μ PLE scan indicating the p-shell. b) Second-order photon autocorrelation function (black dots) and corresponding convoluted fit (blue solid line) revealing an antibunching value of $g^{(2)}(0)_{\text{fit,p-shell}} = (0.12 \pm 0.02)$. c) Fluorescence spectrum under pulsed s-shell resonant excitation. The inset shows the same data in logarithmic intensity-scaling to visualize the remaining scattered laser. d) Second-order photon autocorrelation function and corresponding fit in resonant excitation yielding $g^{(2)}(0)_{\text{fit,s-shell}} = (0.073 \pm 0.005)$.

the used pulse-slicing apparatus is not free of dispersion we typically see a power dependence of the QDs RF similar to an adiabatic rapid passage.^[39] In saturation of the transition (50 nW excitation power), we measure an antibunching value of $g^{(2)}(0)_{\text{fit,s-shell}} = 0.073 \pm 0.005$ (Figure 3d), clearly superior to the value extracted in saturation via p-shell excitation. A change in the temporal dynamics can be seen in the autocorrelation histograms and is confirmed in the exponential decay constant of the correlation peaks, which is reduced from about 2.1 ns under p-shell excitation to 1.4 ns under s-shell excitation. We attribute this observation to the lower density of free charge carriers induced by s-shell resonant excitation, and therefore an also reduced timing jitter. Also, we can see a reduced linewidth of the transition (51 μ eV compared to 62 μ eV in p-shell excitation). While being far above the natural linewidth of a few μ eV, this

states a clear indication of a more coherent driving of the two-level system. We attribute the remaining significant line-broadening when compared to resonant excitation of (001) QDs to structural imperfections of the grown sample, also being reflected in the enhanced resonance fluorescence while adding weak off-resonant pumping. Generally, a statistical measure over 50 QDs of the sample reveals values of excitonic linewidths from 40 to about 120 μ eV, comparable to the average seen in site-controlled (111) QDs, where also values below 25 μ eV have been reported.^[26] The here investigated QD shows a linewidth of about 45 μ eV under off-resonant cw excitation (cf. Figure 2a), yet under pulsed off-resonant excitation (860 nm) the linewidth is identical to the one obtained in p-shell. We explain this by the strong change of photon-induced free carrier density and the related spectral fluctuations when using 2 ps optical pulses.

These promising results in resonant excitation can also be reproduced on a nearby second (111) QD. The off-resonant characteristics are shown in **Figure 4a–c**, revealing two biexcitonic lines as determined from their power dependence and one excitonic state emitting at 1.332 eV, which due to the lack of a clear polarization dependence cannot reliably be identified as a neutral or charged exciton. On this excitonic line, three autocorrelation measurements are carried out under pulsed resonant excitation and the contribution of photons resulting from the off-resonant contribution of the stabilizing white light is investigated (see Figure 4d, e): a) with spectral filtering using the monochromators exit slit (75 μeV bandwidth), b) with a 10 nm bandpass filter centered at 930 nm, and c) without any spectral filtering, directly feeding the entire signal of the detection fiber into the HBT setup. Following the same aforementioned fit procedure, a value of $g^{(2)}(0)_{\text{fit}} = 0.033 \pm 0.027$ is extracted for case (a) (Figure 4d), while the other two measurements show a nonvanishing component at zero time delay (Figure 4e, bandpass) as well as now significantly stronger the aforementioned contribution of the white

light in (Figure 4e, no filtering). The corresponding multi-photon suppression is evaluated first via integrating over equal time intervals of 12.5 ns (corresponding to the excitation pulse separation at 80 MHz) as well as allowing for a background subtraction by adding a baseline to the fit to suppress signal unrelated to the addressed QD transition. This results in integrated values of $g^{(2)}(0)_{\text{bandpass}} = 0.31 \pm 0.02$ and $g^{(2)}(0)_{\text{no-filter}} = 0.56 \pm 0.03$ and background-subtracted single-photon emission of $g^{(2)}(0)_{\text{bandpass}} = 0.062 \pm 0.008$ and $g^{(2)}(0)_{\text{no-filter}} = 0.097 \pm 0.009$. In general, the autocorrelation measurements clearly prove a strong multi-photon suppression, just slightly inferior to other works on (111) site controlled QDs, [26,45] while the (001) oriented substrate still allows for superior values so far.

High photon indistinguishability is a key requirement for on-demand single photons to be applied in advanced quantum technology concepts such as quantum repeater networks. To evaluate this important parameter for the first time for (111) QDs, a Hong–Ou–Mandel (HOM)-type experiment was applied.

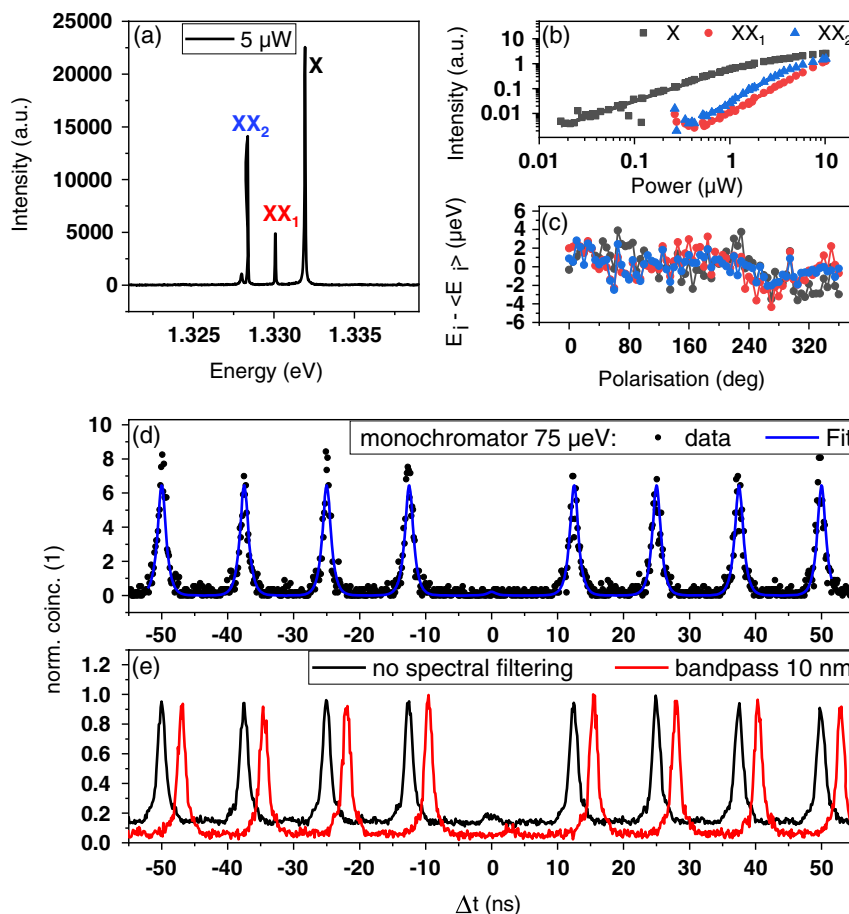


Figure 4. a) Spectrum of a second (111)-QD under off-resonant (785 nm, cw) excitation. b, c): Power- and polarization-dependent characteristics of the three indicated states. Linear fits to the data in b) (solid lines) yield the following values: 1.27 ± 0.06 for X, 2.24 ± 0.04 for XX₁, and 2.07 ± 0.05 for XX₂. d, e): Second-order autocorrelation functions of the excitonic state in pulsed resonance fluorescence: d) Measured histogram using a spectral selection window of $\approx 75 \mu\text{eV}$ yielding an antibunching value of (0.033 ± 0.027) . e) Measured histogram using a 10 nm bandpass filter (red) or no spectral filtering (black). An artificial time difference of 3 ns is introduced for better visibility. The background-subtracted $g^{(2)}(0)$ values are (0.062 ± 0.008) and (0.097 ± 0.009) , respectively.

The setup includes two identical fiber-based asymmetric Mach-Zehnder interferometers (see **Figure 5a**), each of which comprises a delay of 4 ns in one of its arms. One of them is introduced in the excitation line to generate two pulses from the resonant laser and the second in the detection path to overlay two consecutively emitted photons in time and allow for their non-classical interference. Correlating the two outputs the 80 MHz excitation frequency in combination with the 4 ns delay leads to a characteristic pattern in the interferogram as seen in **Figure 5b**. The HOM visibility can be then extracted by comparing the peak at the zero-time delay (A_0) and the adjacent side peaks (A_S): $V_{\text{HOM}} = 1 - (3A_0)/(2\overline{A_S})$, $\overline{A_S}$ being the average of the two peaks. Strict resonant excitation of the first QD gives us a visibility of $V_{\text{HOM}} = (41 \pm 10)\%$. A control measurement is conducted, where the photons are rendered distinguishable by a 90° switch of polarization in one arm (cross-polarized configuration). Our achieved visibility is significantly lower than values exceeding 90% reported for (001) InGaAs QDs and (001) GaAs QDs.^[3,8,18–22,40] Still, the achieved indistinguishability, together with the high multi-photon suppression, demonstrates the general potential of (111) QDs to act as high-quality quantum emitters. It also indicates that further material and subsequent

device optimization is necessary to improve the quantum nature of emission. Related studies could focus on optimized epitaxial growth to further reduce the emission linewidth by a lower defect density. In addition, it will be interesting to integrate (111) QDs into cavity structures, like CBGs, to increase the photon indistinguishability by employing light-matter coupling effects.^[20,33–35]

4. Conclusion

In conclusion, we reported on the epitaxial growth of InGaAs QDs with backside DBR mirror on (111)-oriented GaAs substrate and performed optical and quantum optical studies to evaluate the potential of these structures to act as two-level emitters in the field of photonic quantum technologies. The highest crystal quality was obtained using n-doped (111)B GaAs substrate, with a miscut of 2° in the [211] direction. Utilizing MBE-grown high-quality QD heterostructures based on such a substrate, we performed detailed optical investigations under non-resonant, quasi-resonant, and to our best knowledge for the first time also strict resonant excitation. Best results in terms of emission linewidth, multi-photon suppression, and photon indistinguishability were obtained in resonance fluorescence when exciting directly into the s-shell of the (111) QD. Our results demonstrate that the studied (111) QDs act as promising two-level emitters which, due to their typically small fine structure splitting, could be interesting candidates for the realization of bright polarization-entangled photon-pair sources in the future. However, the determined HOM visibility of $(41 \pm 10)\%$ also indicates that additional growth and also device optimization is necessary to reach values >90% achieved for mature (001) InGaAs and (001) GaAs QDs and to utilize the full potential of (111) QDs in the field of photonic quantum technologies.

Acknowledgements

The authors acknowledge support from the German Research Foundation (DFG) via Grant RE2974/12–1, from the Russian Foundation for Basic Research, project no. 16-52-12023, and from the project EMPIR JRP 17FUN06 SIQUST (the EMPIR initiative is co-funded by the European Union's Horizon 2020 research and innovation program and the EMPIR Participating States). The authors further acknowledge technical support by the group of Tobias Heindel funded via the BMBF project “QuSecure” (Grant No. 13N14876) within the funding program Photonic Research Germany.

Open Access funding enabled and organized by Projekt DEAL.

Conflict of Interest

The authors declare no conflict of interest.

Data Availability Statement

The data that support the findings of this study are available from the corresponding author upon reasonable request.

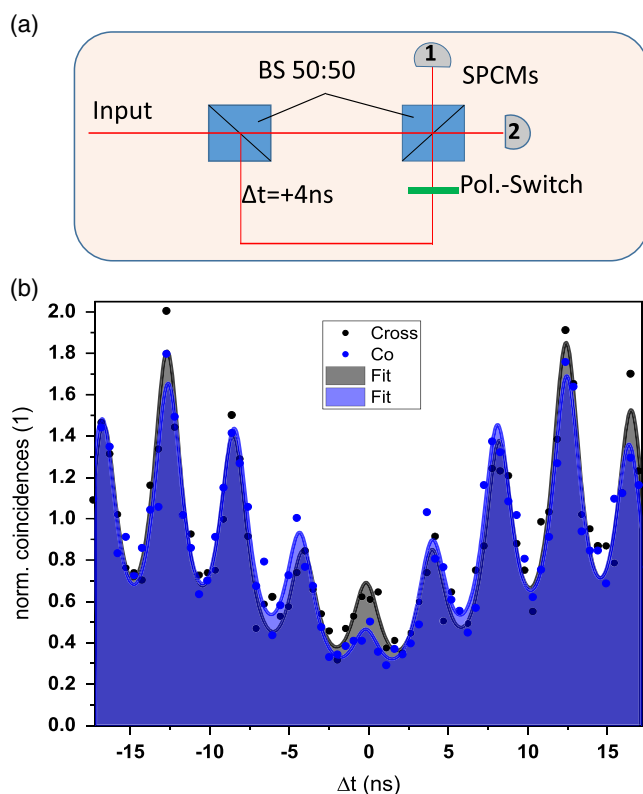


Figure 5. a) For the Hong–Ou–Mandel experiment, a fiber-based asymmetric Mach Zehnder interferometer is introduced to the excitation and detection path. It adds a 4 ns delay to one arm, which includes an adjustable 0°/90° polarization switch. b) Interferogram of the strict-resonantly excited QD in HOM configuration for co- and cross-polarized settings. Fitting of the experimental data yields a visibility of $V_{\text{HOM}} = (41 \pm 10)\%$.

Keywords

indistinguishability, quantum dots, resonance fluorescence, single-photon emission, (111)-GaAs

Received: April 8, 2022

Revised: May 16, 2022

Published online: June 19, 2022

- [1] S.-K. Liao, W.-Q. Cai, W.-Y. Liu, L. Zhang, Y. Li, J.-G. Ren, J. Yin, Q. Shen, Y. Cao, Z.-P. Li, F.-Z. Li, X.-W. Chen, L.-H. Sun, J.-J. Jia, J.-C. Wu, X.-J. Jiang, J.-F. Wang, Y.-M. Huang, Q. Wang, Y.-L. Zhou, L. Deng, T. Xi, L. Ma, T. Hu, Q. Zhang, Y.-A. Chen, N.-L. Liu, X.-B. Wang, Z.-C. Zhu, C.-Y. Lu, et al., *Nature* **2017**, 549, 43.
- [2] T. Kupko, M. von Helversen, L. Rickert, J.-H. Schulze, A. Strittmatter, M. Gschrey, S. Rodt, S. Reitzenstein, T. Heindel, *NPJ Quantum Inf.* **2020**, 6, 1.
- [3] F. B. Basset, M. Valeri, E. Roccia, V. Muredda, D. Poderini, J. Neuwirth, N. Spagnolo, M. B. Rota, G. Carvacho, F. Sciarrino, R. Trotta, *Sci. Adv.* **2021**, 7, 12.
- [4] C. Schimpf, M. Reindl, D. Huber, B. Lehner, S. F. C. da Silva, S. Manna, M. Vylecka, P. Walther, A. Rastelli, *Sci. Adv.* **2021**, 7, 16.
- [5] M. Reindl, D. Huber, C. Schimpf, S. F. C. da Silva, M. B. Rota, H. Huang, V. Zwiller, K. D. Jöns, A. Rastelli, R. Trotta, *Sci. Adv.* **2018**, 4, 12.
- [6] M. Anderson, T. Müller, J. Huwer, J. Skiba-Szymanska, A. Krysa, R. Stevenson, J. Heffernan, D. Ritchie, A. Shields, *NPJ Quantum Inf.* **2020**, 6, 1.
- [7] J. B. Spring, B. J. Metcalf, P. C. Humphreys, W. S. Kolthammer, X.-M. Jin, M. Barbieri, A. Datta, N. Thomas-Peter, N. K. Langford, D. Kundys, J. C. Gates, B. J. Smith, P. G. R. Smith, I. A. Walmsley, *Science* **2012**, 339, 798.
- [8] J. C. Lored, M. A. Broome, P. Hilaire, O. Gazzano, I. Sagnes, A. Lemaitre, M. P. Almeida, P. Senellart, A. G. White, *Phys. Rev. Lett.* **2017**, 118, 130503.
- [9] H. Wang, Y. He, Y.-H. Li, Z.-E. Su, B. Li, H.-L. Huang, X. Ding, M.-C. Chen, C. Liu, J. Qin, J.-P. Li, Y.-M. He, C. Schneider, M. Kamp, C.-Z. Peng, S. Höfling, C.-Y. Lu, J.-W. Pan, *Nat. Photonics* **2017**, 11, 361.
- [10] H. Wang, J. Qin, X. Ding, M.-C. Chen, S. Chen, X. You, Y.-M. He, X. Jiang, L. You, Z. Wang, C. Schneider, J. Renema, S. Höfling, C.-Y. Lu, J.-W. Pan, *Phys. Rev. Lett.* **2019**, 123, 250503.
- [11] A. Dibos, M. Raha, C. Phenicie, J. D. Thompson, *Phys. Rev. Lett.* **2018**, 120, 243601.
- [12] P. Lombardi, M. Colautti, R. Duquennoy, G. Murtaza, P. Majumder, C. Toninelli, *Appl. Phys. Lett.* **2021**, 118, 204002.
- [13] D. Riedel, I. Söllner, B. J. Shields, S. Starosielec, P. Appel, E. Neu, P. Maletinsky, R. J. Warburton, *Phys. Rev. X* **2017**, 7, 031040.
- [14] G. Juska, E. Murray, V. Dimastrodonato, T.-H. Chung, S. T. Moroni, A. Gocalinska, E. Pelucchi, *J. Appl. Phys.* **2015**, 117, 134302.
- [15] S. Bounouar, C. de la Haye, M. Strauß, P. Schnauber, A. Thoma, M. Gschrey, J.-H. Schulze, A. Strittmatter, S. Rodt, S. Reitzenstein, *Appl. Phys. Lett.* **2018**, 112, 153107.
- [16] D. Huber, M. Reindl, S. F. C. da Silva, C. Schimpf, J. Martín-Sánchez, H. Huang, G. Piredda, J. Edlinger, A. Rastelli, R. Trotta, *Phys. Rev. Lett.* **2018**, 121, 033902.
- [17] M. Rezaei, J. Wrachtrup, I. Gerhardt, *Optica* **2019**, 6, 34.
- [18] N. Somaschi, V. Giesz, L. D. Santis, J. C. Lored, M. P. Almeida, G. Hornecker, S. L. Portalupi, T. Grange, C. Antón, J. Demory, C. Gómez, I. Sagnes, N. D. Lanzillotti-Kimura, A. Lemaitre, A. Auffeves, A. G. White, L. Lanco, P. Senellart, *Nat. Photonics* **2016**, 10, 340.
- [19] E. Schöll, L. Hanschke, L. Schweickert, K. D. Zeuner, M. Reindl, S. F. C. da Silva, T. Lettner, R. Trotta, J. J. Finley, K. Müller, A. Rastelli, V. Zwiller, K. D. Jöns, *Nano Lett.* **2019**, 19, 2404.
- [20] J. Liu, R. Su, Y. Wei, B. Yao, S. F. C. da Silva, Y. Yu, J. Iles-Smith, K. Srinivasan, A. Rastelli, J. Li, X. Wang, *Nat. Nanotechnol.* **2019**, 14, 586.
- [21] H. Wang, H. Hu, T.-H. Chung, J. Qin, X. Yang, J.-P. Li, R.-Z. Liu, H.-S. Zhong, Y.-M. He, X. Ding, Y.-H. Deng, Q. Dai, Y.-H. Huo, S. Höfling, C.-Y. Lu, J.-W. Pan, *Phys. Rev. Lett.* **2019**, 122, 11.
- [22] N. Tomm, A. Javadi, N. O. Antoniadis, D. Najer, M. C. Löbl, A. R. Korsch, R. Schott, S. R. Valentin, A. D. Wieck, A. Ludwig, R. J. Warburton, *Nat. Nanotechnol.* **2021**, 16, 399.
- [23] A. Schliwa, M. Winkelnkemper, A. Lochmann, E. Stock, D. Bimberg, *Phys. Rev. B* **2009**, 80, 161307.
- [24] K. Karlsson, M. Dupertuis, D. Oberli, E. Pelucchi, A. Rudra, P.-O. Holtz, E. Kapon, *Phys. Rev. B* **2010**, 81, 161307.
- [25] O. Benson, C. Santori, M. Pelton, Y. Yamamoto, *Phys. Rev. Lett.* **2000**, 84, 2513.
- [26] I. R. Jahromi, G. Juska, S. Varo, F. B. Basset, F. Salusti, R. Trotta, A. Gocalinska, F. Mattana, E. Pelucchi, *Appl. Phys. Lett.* **2021**, 118, 073103.
- [27] L. Schweickert, K. D. Jöns, K. D. Zeuner, S. F. C. da Silva, H. Huang, T. Lettner, M. Reindl, J. Zichi, R. Trotta, A. Rastelli, V. Zwiller, *Appl. Phys. Lett.* **2018**, 112, 093106.
- [28] A. Fognini, A. Ahmadi, M. Zeeshan, J. T. Fokkens, S. J. Gibson, N. Sherlekar, S. J. Daley, D. Dalacu, P. J. Poole, K. D. Jöns, V. Zwiller, M. E. Reimer, *ACS Photonics* **2019**, 6, 1656.
- [29] D. Huber, M. Reindl, Y. Huo, H. Huang, J. S. Wildmann, O. G. Schmidt, A. Rastelli, R. Trotta, *Nat. Commun.* **2017**, 8, 1.
- [30] J. Zhang, J. S. Wildmann, F. Ding, R. Trotta, Y. Huo, E. Zallo, D. Huber, A. Rastelli, O. G. Schmidt, *Nat. Commun.* **2015**, 6, 1.
- [31] O. Gazzano, S. Michaelis de Vasconcellos, C. Arnold, A. Nowak, E. Galopin, I. Sagnes, L. Lanco, A. Lemaitre, P. Senellart, *Nat. Commun.* **2013**, 4, 1.
- [32] S. Unsleber, Y.-M. He, S. Gerhardt, S. Maier, C.-Y. Lu, J.-W. Pan, N. Gregersen, M. Kamp, C. Schneider, S. Höfling, *Opt. Express* **2016**, 24, 8539.
- [33] H. Wang, Y.-M. He, T.-H. Chung, H. Hu, Y. Yu, S. Chen, X. Ding, M.-C. Chen, J. Qin, X. Yang, R.-Z. Liu, Z.-C. Duan, J.-P. Li, S. Gerhardt, K. Winkler, J. Jurkat, L.-J. Wang, N. Gregersen, Y.-H. Huo, Q. Dai, S. Yu, S. Höfling, C.-Y. Lu, J.-W. Pan, *Nat. Photonics* **2019**, 13, 770.
- [34] M. Moczala-Dusanowska, Ł. Dusanowski, O. Iff, T. Huber, S. Kuhn, T. Czyszanowski, C. Schneider, S. Höfling, *ACS Photonics* **2020**, 7, 3474.
- [35] S. Kolatschek, C. Nawrath, S. Bauer, J. Huang, J. Fischer, R. Sittig, M. Jetter, S. L. Portalupi, P. Michler, *Nano Lett.* **2021**, 21, 7740.
- [36] M. Gschrey, A. Thoma, P. Schnauber, M. Seifried, R. Schmidt, B. Wohlfeil, L. Krüger, J. H. Schulze, T. Heindel, S. Burger, F. Schmidt, A. Strittmatter, S. Rodt, S. Reitzenstein, *Nat. Commun.* **2015**, 6, 7662.
- [37] I. A. Derebezov, V. A. Gaisler, A. V. Gaisler, D. V. Dmitriev, A. I. Toropov, M. von Helversen, C. de la Haye, S. Bounouar, S. Reitzenstein, *Semiconductors* **2019**, 53, 1304.

- [38] A. V. Kuhlmann, J. Houel, D. Brunner, A. Ludwig, D. Reuter, A. D. Wieck, R. J. Warburton, *Rev. Sci. Instrum.* **2013**, *84*, 7.
- [39] Y.-J. Wei, Y.-M. He, M.-C. Chen, Y.-N. Hu, Y. He, D. Wu, C. Schneider, M. Kamp, S. Höfling, C.-Y. Lu, J.-W. Pan, *Nano Lett.* **2014**, *14*, 11.
- [40] Y.-M. He, Y. He, Y.-J. Wei, D. Wu, M. Atatüre, C. Schneider, S. Höfling, M. Kamp, C.-Y. Lu, J.-W. Pan, *Nat. Nanotechnol.* **2013**, *8*, 213.
- [41] T. Kaldewey, S. Lüker, A. V. Kuhlmann, S. R. Valentin, A. Ludwig, A. D. Wieck, D. E. Reiter, T. Kuhn, R. J. Warburton, *Phys. Rev. B* **2017**, *95*, 161302.
- [42] M. Strauß, A. Kaganskiy, R. Voigt, P. Schnauber, J.-H. Schulze, S. Rodt, A. Strittmatter, S. Reitzenstein, *Appl. Phys. Lett.* **2017**, *110*, 111101.
- [43] H. S. Nguyen, G. Sallen, C. Voisin, P. Roussignol, C. Diederichs, G. Cassaboïs, *Phys. Rev. Lett.* **2012**, *108*, 057401.
- [44] O. Gazzano, T. Huber, V. Loo, S. Polyakov, E. Flagg, G. Solomon, *Optica* **2018**, *5*, 354.
- [45] M. A. M. Versteegh, M. E. Reimer, A. A. van den Berg, G. Juska, V. Dimastrodonato, A. Gocalinska, E. Pelucchi, V. Zwiller, *Phys. Rev. A* **2015**, *92*, 033802.